Ellipsometric and Cyclic Voltammetric studies of Corrosion of Carbon Steel in K_2SO_4 Solution in presence of $NaNO_2$

P. R. SINGH, P. K. CHAUHAN & H. S. GADIYAR
Metallurgy Division, B.A.R.C. Bombay

CORROSION behaviour of carbon steel and the characteristics of the film formed on its surface in K_2SO_4, $NaNO_2$ and K_2SO_4 + $NaNO_2$ solutions were studied by direct weight loss, cyclic voltammetry and ellipsometry.

Direct weight loss measurements have shown corrosion inhibition efficiency of ~ 99% in 200 ppm $NaNO_2$ solution and about 88% in a solution containing a mixture of 800 ppm $NaNO_2$ and 400 ppm K_2SO_4.

Cyclic voltammetry was carried out between -1600 mV and +800 mV (vs. SCE) in 400 ppm K_2SO_4, 800 ppm $NaNO_2$ and 400 ppm K_2SO_4 + 800 ppm $NaNO_2$ solutions. The steel dissolved freely in K_2SO_4. In $NaNO_2$ and K_2SO_4 + $NaNO_2$ solutions, the voltammetric behaviour was similar. Three peaks appeared on the anodic cycle while two on the cathodic cycle. The voltammogram showed high degree of polarization.

From ellipsometric measurements in 100 and 200 ppm $NaNO_2$, the film refractive index was found to be 1.69 (1-0.0i). The film thicknesses were 29.0 Å and 25.5 Å after 4 hours of exposure. In case of K_2SO_4 + $NaNO_2$ solutions the film was found to have the refractive index of 1.63 (1-0.03i) with a thickness of 71.8 Å in 24 hours. The results suggest that in presence of $NaNO_2$, corrosion of mild steel in K_2SO_4 solution is inhibited by the formation of passive FeO(OH) layer.

CARBON steels are widely accepted construction materials for most of the water recirculating systems. As such, the corrosion behaviour of these steels is of primary interest. Corrosion of iron has been studied extensively under a variety of conditions[1-6]. Still, the nature of the corrosion products, passivating layer formed under different conditions and the various corrosion mechanisms have been a a subject of discussion. Recently, several attempts have been made to rationalise the action of inhibitors on iron and steel in terms of film thickness and composition as obtained from optical and electrochemical methods[7-11]. The present study deals with aqueous medium and some aspects of inhibition by $NaNO_2$ in K_2SO_4 solutions. Nitrites, which are effective in aerated as well as in deaerated neutral solutions belong to the oxidising type of corrosion inhibitors. This study includes inhibition due to $NaNO_2$ in K_2SO_4 by weight loss method, cyclic voltammetry and ellipsometry.

EXPERIMENTAL

The steel specimens used in these investigations were of the following composition :C – 0.11%, Mn – 0.35%, P – 0.03%, S – 0.03% and Si – 0.04%. All the solutions were prepared from AR grade chemicals in double distilled water. The corrosion rates were determined by direct weight loss method.

Cyclic voltammetric measurements were carried out using three electrode polarization cell with SCE (with a luggin probe) as the reference electrode and platinum counter electrode. The specimen electrode was of cylindrical shape (~ 1 cm^2 area). Distance between the luggin probe and the working electrode was maintained at 2-3 mm.

Ellipsometric measurments were carried out on rectangular coupons of dimensions 21 mm × 17 mm × 2 mm using Gaertner Elipsometer Model L 119X. The specimens were polished with diamond paste to have bright mirror surfaces. Mercury green light (5461 Å) was allowed to fall on the specimens at 60° angle of incidence. Initially, optical constants of a film free surface were determined by holding the specimen at – 1600 mV/SCE for one hour and recording the elliposmetric readings. The specimen was then allowed to attain the rest potential and film growth was followed for 24 hours. The film characteristics were studied in 100 and 200 ppm $NaNO_2$ and in 400 ppm K_2SO_4 + 800 ppm $NaNO_2$.

RESULTS

Weight Loss Data : Table 1 shows the results of weight loss experiments. About 99% inhibition efficiency can be seen in presence of $NaNO_2$ in

TABLE 1

Corrosion Inhibition Efficiency of $NaNO_2$ for Mild Steel in Aqueous Solution

Medium	Corrosion Rate mg/dm²/day	Inhibition Efficiency %
D.D. Water	22.6	—
200 ppm $NaNO_2$	0.021	99.9
400 ppm K_2SO_4 + 800 ppm $NaNO_2$	2.67	88.2

plain double distilled water. In sulphite-nitrite mixture, it is about 88%.

Cyclic Voltammetry : Cyclic voltammetry was carried out in three solutions viz. 400 ppm K_2SO_4, 800 ppm $NaNO_2$ and 400 ppm K_2SO_4 + 800 ppm $NaNO_2$. Reproducibility of the voltammograms could be improved either by scanning the potential between −1600 mV and + 800 mV for 20 minutes at a high scan rate (300 mV/sec) or by holding the potential at −1600 mV for > 10 minutes. Both the procedures were adopted.

In case of 400 ppm K_2SO_4 (Fig. 1), steady dissolution was observed. Reversed hysteresis was obsereved at the lower scan rates (3 and 10 mV/sec) on the anodic side of the rest potential (−500 mV). There was no pitting on the specimen surface. The reverse hysteresis may arise from some potential dependent adsorption process. On the cathodic cycle (at 10 mV/sec), there was a plateau between −660 mV and −780 mV and a peak at −1150 mV. The platen may result from oxygen reduction. The cathodic peak may result from reduction of some adherent oxide. Optical examination of the surface revealed only partial coverage. On the whole, corrosion products were loose.

Cyclic voltametric behaviour of carbon steel in 400 ppm K_2SO_4 + 800 ppm $NaNO_2$ and 800 ppm $NaNO_2$ solutions was similar. The results in sulphate-nitrite solution only are given here. The rest potential in this solution was −340 mV. Fig. 2 shows the voltammograms at a scan rate of 10 mV/sec in K_2SO_4 and K_2SO_4 + $NaNO_2$ solutions. In presence of $NaNO_2$, the reverse hysteresis which was prominent in the solution containing K_2SO_4 alone, did not appear. Three anodic peaks appeared

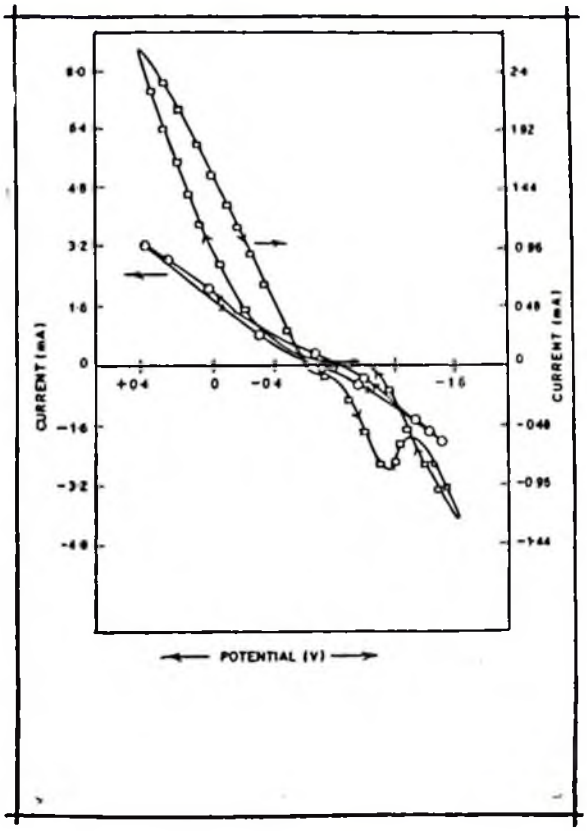


Fig. 1 Cyclic voltammograms of carbon steel in 400 ppm K_2SO_4 solution, electrode area = 0.73 cm². —0—300 mV/sec., —□—10 mV/sec.

along with one cathodic peak. At very low scan rate, one additional peak appeared on the anodic cycle.

Fig. 3 shows the repetitive cyclic voltammogram in $NaNO_2$ − K_2SO_4 solution between −1600 mV and + 800 mV/sec. Arrows show the direction of shift of peaks. In the first cycle, four peaks (I, II' III and IIIa) were observed on the anodic cycle along with a plateau (X) and a peak (V) on the cathodic cycle. Peak IIIa appears as a shoulder of peak III. In the subsequent cycling, peak I remained constant, II decreased slightly, while III increased in height and shifted in anodic direction. Peak IIIa disappeared (decreased) but another peak (IV) appeared at + 50 mV. It increased in peak height and shifted anodically. On the cathodic side, plateau (X) remained constant but peak (V) increased in height and shifted in cathodic direction. After about 32 cycles, the system reached steaey state.

Fig. 4 shows the effect of anodic potential limit E_{la} on the voltammogram at 30 mV/sec. This

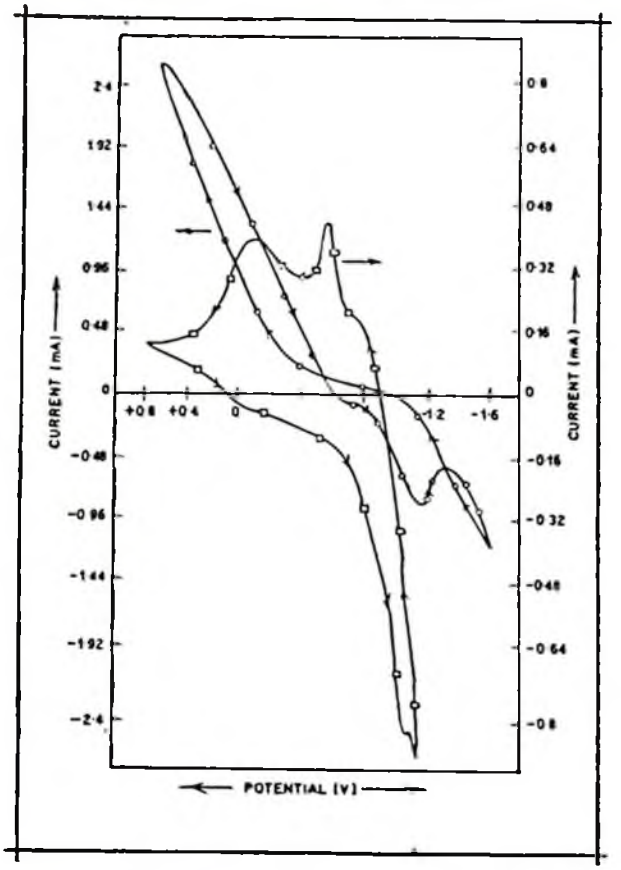


Fig. 2 Cyclic voltammograms of carbon steel at 10 mV/sec. area 0.73 cm². —0— 400 ppm K_2SO_4, —□— 400 ppm K_2SO_4 + 800 ppm $NaNO_2$.

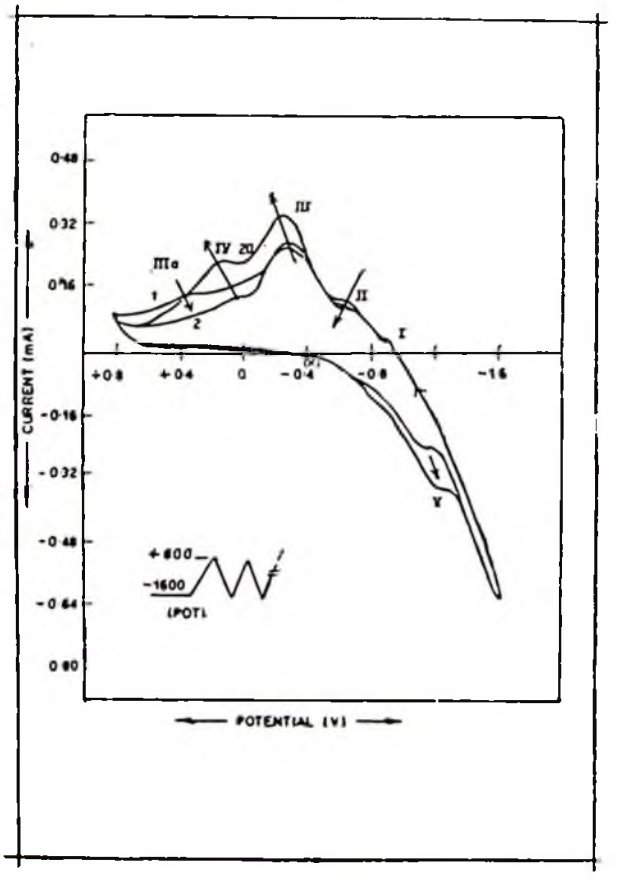


Fig. 3 Reptitive cyclic voltammogram of carbon steel in 400 ppm K_2SO_4 + 800 ppm $NaSO_4$. Scan rate 100 mV/sec. Area 1.07 cm².

was done in order to trace the origin of cathodic peak V. It appears that it arises due to reduction of product formed at peak III. Effect of cathodic potential limit E_{1c} is shown in fig. 5. Initially E_{1c} was kept at −1600 mV. It was increased in subsequent cycles, the increment being 50 mV per cycle. At $E_{1c} < -1350$ mV, peak I and II were unchanged. Al $E_{1c} > -1350$, I and II disappeared in the same order. For $E_{1c} > -1100$ mV, drastic reduction in peak III occurred which became more prominent for $E_{1c} > -900$ mV. At $E_{1c} > -800$ mV, peak III disappeared. Peak IV first decreased followed by increase for E_{1c} ranging from −1300 mV to −950 mV.

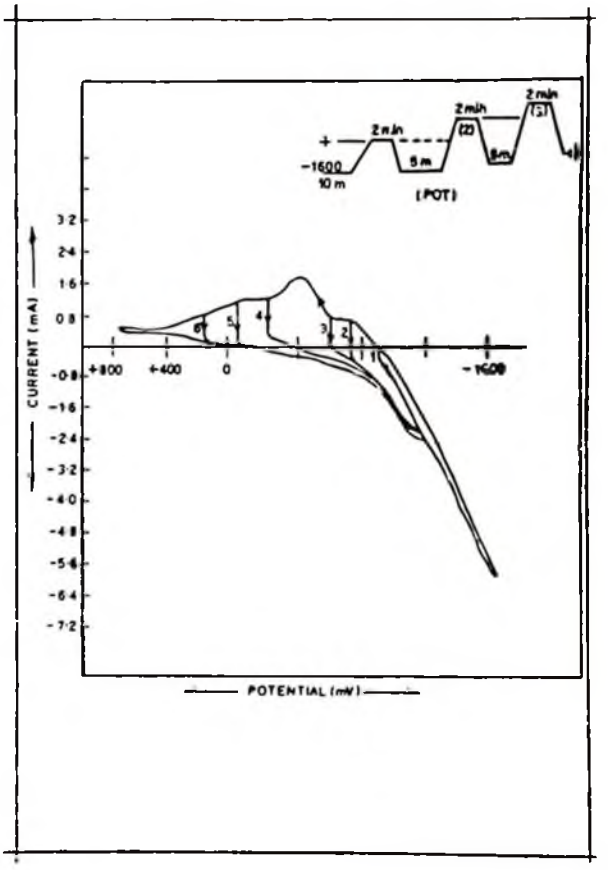


Fig. 4 Effect of anodic potential limit E_{1a} on cyclic voltammogram of carbon steel in 400 ppm K_2SO_4 + 800 ppm $NaNO_2$. Scan rate 30 mV/sec. Area 1.104 cm².

Fig. 6. represents the effect of scan rate on the voltammograms. At the scan rate of 3 mV/sec, the current scale has been changed at points B and A. The corresponding scales have been given on the right side of the graph. The anodic currents are referred to B while the cathodic to A. At high scan rates, only one anodic peak appeared. At 3 and 10 mV/sec, all four anodic speaks (I, II, III and IV) appeared clearly alongwith two plateaus and one cathodic peak. At 10 mV/sec, peak IIIa appeared as a distorted shoulder of peak III. Peak IV became most prominent at 3 mV/sec. In fig. 7, the effect

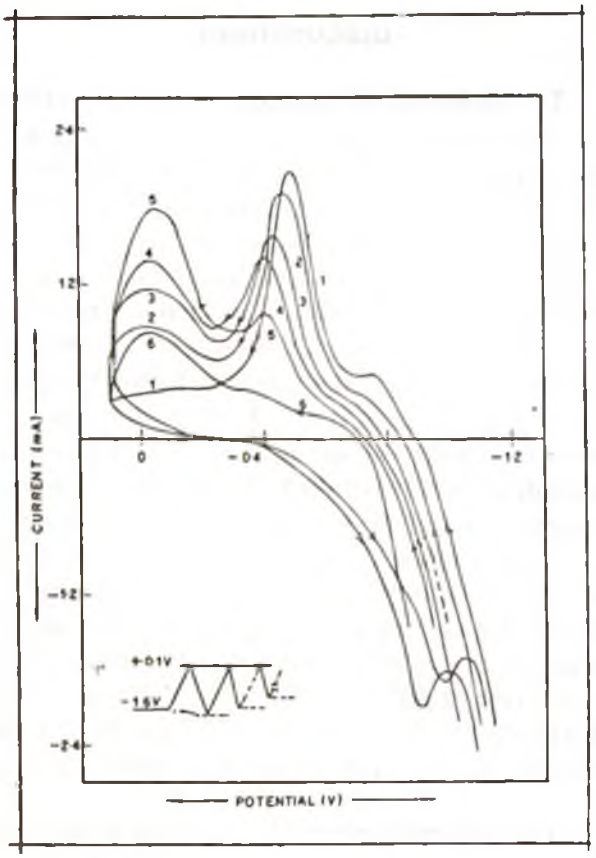


Fig. 5 Effect of cathodic potential limit E_{lc} on the cyclic voltammogram of carbon steel in 400 ppm K_2SO_4 + 800 ppm $NaNO_3$. Scan rate 30 mV/sec. Area 1.62 cm^2.

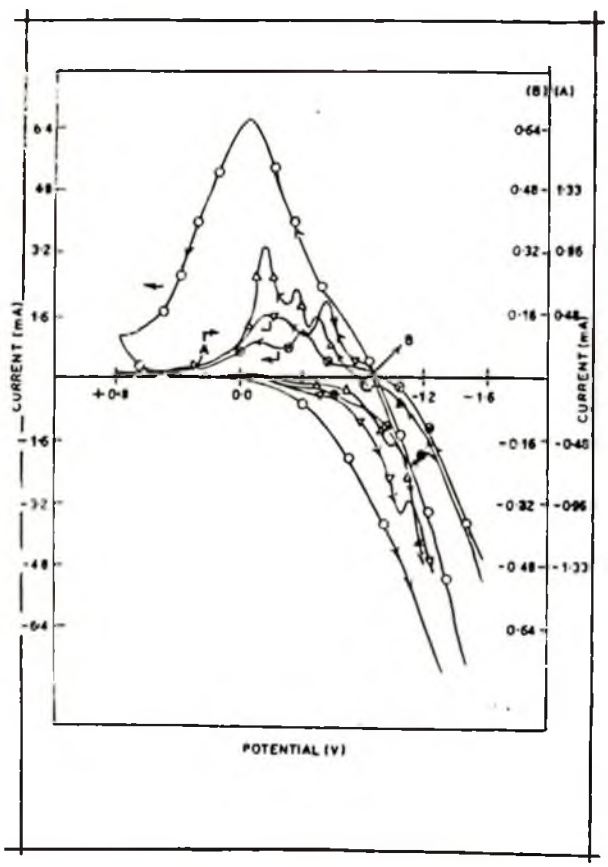


Fig. 6 Effect of scan rate on cyclic voltammogram of carbon steel in 400 ppm K_2SO_4 + 800 ppm $NaNO_3$. Area 1.1 cm^2. —0—300,— × —30,— ▽ —10,— △ —3 mV/sec.

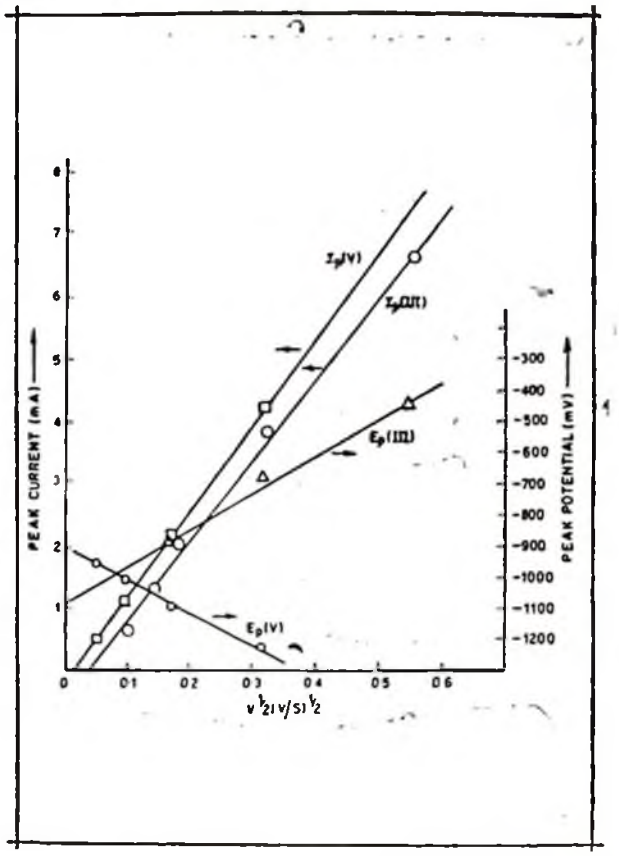


Fig. 7. Dependence of peak potential (E_p) and peak current (i_p) on scan rate, of carbon steel in 400 ppm K_2SO_4 + 800 ppm $NaNO_3$.

of scan rates on peak potential 'E_p' and peak current 'i_p' has been shown. Peaks I and II don't seem to be very clear. Peak III and V were examined more closely. These two peaks follow each other in the change of E_p and i_p. The dependence of E_p and i_p of these two peaks are closest to $E_p - V^{\frac{1}{2}}$ and $i_p - V^{\frac{1}{2}}$ straight line curves.

Ellipsometry : The optical constants of the bare carbon steel specimen were obtained in K_2SO_4-$NaNO_3$ solution by holding the specimen at -1600m V/SCE for one hour. Δ and ψ values obtained at this potential were used to obtain the complex refractive index for the bare surface. The obtained value of 2.98 (1-1.2i) was slightly less than the value reported in literature[9]. Using this value for the substrate refractive index, McCrackin's Computer Program[12] was employed to calculate a series of Δ ane ψ values for the films of various refractive indices and thicknesses. Initially, thickness range was set at 0-100A° and the film refractive index ($\bar{n}_1$) was varied between 1.5 (1-0i) and 3.5 (1-0.5i) to allow for the maximum range of this parameter for bulk iron oxides reported in literature[13-18]. Computational chart of Δ vs ψ for the films of various refractive indices were prepared. The

experimental $\Delta-\psi$ curves were compared with the theoretical ones to find out the refractive indices and thicknesses of oxide films,

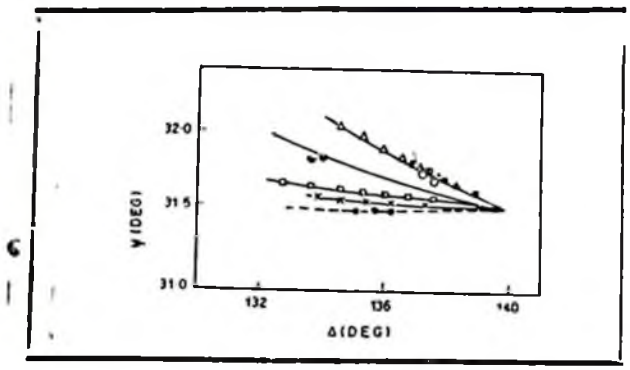


Fig. 8. Ellipsometric Results

Theoretical $\Delta-\psi$ curves for various refractive indices ($\bar{n}_f$ —△—1.7 (1-0.0i),—1.6 (1.0.25i),—□—□—2.5 (1-0.025i),————1.7 (1-0.07i) and—×-×-×—1.6 (1-0 05i).

Experimental points in● 400 ppm K SO + 800 ppm $NaNO_2$ □100 ppm $NaNO_2$ and —0—200 ppm $NaNO_2$.

Fig. 8 shows the computational as well as well as experimental $\Delta-\psi$ plots. It appears that the initial film in K_2SO_4-$NaNO_2$ solu ion had a refractive index ~ 1.7 (1-0.075i) which changed to 1.6 (1-0.025i) after 24 hours. The exact values were calculated by feeding approximate data to computer. The film thickness grows upto 71.8 Å in 24 hours. In 100 ppm $NaNO_2$ solution, the film refractive Index was 1.7 (1-0.0i), its thickness being 29 A° in 4 hours. In 200 ppm $NaNO_2$, the refractive index of the film was the same while thickness remained 25.5 Å in 4 hours. There was no further increase in the film thickness in last two cases (fig. 9).

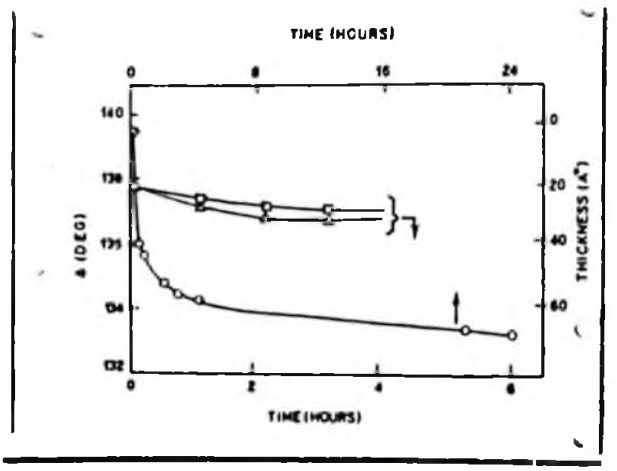


Fig. 9. Relation between △. film thickness and time in —□—200 ppm $NaNO_2$—△—100 ppm $NaNO_2$ and —0— K_2SO_4 + 800 ppm $NaNO_2$.

DISCUSSIONS

The potential for crossing over from cathodic to anodic current was more cathodic to the open circuit potential of carbon steel in K_2SO_4-$NaNO_2$ solution. From this fact and the shape of the overall cyclic voltammograms in K_2SO_4 and K_2SO_4 + $NaNO_2$ solutions, it is obvious that the corrosion inhibition by $NaNO_2$ involves formation of some passive film. The film formed in 100 and 200 ppm $NaNO_2$ solutions was non absorbing with a refractive index of 1 69 (1-0.0i). In sulphate-nitrite mixture it was slightly absorbing with refractive index of 1.63 (1-0.03i). These values are close to those reported by Smialowska et al.[9] and Ho et al.[15]. The former suggested the formation of γ-Fe_2O_3 or Fe_3O_4 while the latter ascribed this value to FeO (OH). The refractive index of the film in the percent case suggests the absence of Fe_3O_4 (n_f = 2.39 (1-0.10i)[16]; 2.50 (1-0.12i)[17] aad Fe_2O_3 (n_f = 2.88 (1-013i)[16]; 3 20 (1-0.3i)[18]. It might be possible that it is mainly FeO(OH) with som hydroxide.

If it is assumed that the passive film at the open circuit potential is FeO(OH), its thickness may be estimated for the charge under the current peak III usrng the relation[19]

$$d = \frac{M}{nFA\theta\rho V}\int_{E_o}^{E_p} idE$$

derived from Faraday's laws. Here d is the film thickness, M its molecular weight (88.85 for FeO (OH)), A, the electrode area (~ 1 cm^2), F = 26500 coulombs, n the number of elect on transferred, θ the surface coverage (~ 0.9), ρ the film meterial density (5 gm/ml^3), V the scan rate. E_i the equalibrium potential and E_p the peak potential With appropriate values of the various parameters, this relation gave the film thicknesses of 43.7 A°, 50 A° 46-50 A° and 34 A° at the voltage scan rates of 10, 30, 100 and 300 mV/sec. respectively. These are in fair agreement with the thickness value obtained by ellipsometry.

Anodic peaks I and II can be attributed to the formation and growth of $Fe(OH)_2$ from Fe(OH) ads., According Guzman et al.[20], the second peak appears because of three dimentional growth of $Fe(OH)_2$ while the first arises as a result of its nucleation.

Peaks III, IV and V are under non equilibrium conditions and also related to one another. III is attributed to formation of FeO(OH). From fig. 5, it is evident that it is partially dependent on peak II. This indicates that formation of FeO(OH) from Fe involves parallel routes as suggested by MacDonald[6] i.e. directly from Fe^o as well through Fe^{++}. By consideration of equilibrium potential, both of these routes are probable.

Peak IV is peculiar in the sense that it becomes more prominent at lower scan rates or in subsequent cycles in repetitive cyclic voltametry. Also it depends on the state of peak III as shown in fig. 5. Guzman et al.[20] have explained this in terms of ageing effect on FeO(OH). According to him, this peak arises due to conversion of δ-FeO(OH) to α-form.

The linear relation between i_p anV$^{\frac{1}{2}}$ suggests a a diffusion controlled process. The i_p vs $V^{\frac{1}{2}}$ curves did not pass through the origin but cut the $V^{\frac{1}{2}}$ axis. Such observation has been reported by Ogura et al.[3-5] for iron under different circumstances. This indicates that some induction period is required for the reaction. Ogura et al.[4] have described such phenomena to an initial charge transfer controlling stage which ultimately becomes diffusion controlled. There should have been another reduction peak for $Fe(OH)_2$ to Fe^o. The repetitive scanning with different cathodic potential limit E_{lc} shows that the reduction of $Fe(OH)_2$ occurs at potentials ≤ -1300 mV. The absence of this peak is because of its overlapping with hydrogen evolution reaction. The surface film had catalytic effect on hydrogen evolution.

It may be concluded that $NaNO_2$ is highly effective corrosion inhibitor for carbon steel in plain double distilled water as well as K_2SO_4 solution. The inhibition is due to formation of passive FeO (OH) film on the surface. The film may contain some amount of $Fe(OH)_2$. The presence of Fe_2O_3 and Fe_3O_4 is ruled out on the basis of refractive index of the surface film.

ACKNOWLEDGEMENT

The authors are thankful to Shri C. V. Sundaram, Head, Metallurgy Division for his keen interest and encouragement shown during these investigations. They wish to record their appreciation to Shri V. K. Kelkar, Chemistry Division, for his help n modifying the computer program for analysis of ellipsometric data.

REFERENCES

1. I. Epelboin and M. Keddam, J. *Electrochem. Soc.*, 117 (1970) 1052.
2. H. C. Kuo and D. Landolt, *Electrochim. Acta*, 20 (1975) 393.
3. K. Ogura and T. Majima, *ibid.*, 23 (1978) 1361.
4. K. Ogura and K. Sato, *ibid.*, 25 (1978) 857.
5. K. Ogura and K Sato, Passivity of Merals, The 4th International Symposium on Passivity (Ed. R. P. Frankenthal, J. Kruger) *Electrochemical Soc.* 1978.
6. D. D. MacDonald and D. Owen, J. *Electrochem. Soc.*, 120 (1973) 317.
7. G. J. Bignold, *Corros. Sci.*, 12 (1972) 145.
8. C. Lukac, J. B. Lumsden, S. Smialowska and R.W. Staehle, *J. Electrochem. Soc.*, 122 (1975) 1671.
9. Z. Smialowska and R. W. Staehle, *ibid.*, 121 (1974) 1146; *ibid.*, 121 (1974) 1393.
10. J. Kruger and J. P. Calvert, *J. Electrochem. Soc.*, 114 (1967) 43.
11. J. B. Lumsden and Z. Smialowska, Corrosion (NACE), 34 (1978) 169.
12. F. L. McCrakin, National Bureau of Standards, *Technical Note* 479 U. S. Government Printing Office, Washington D. C. (1969).
13. G. Lewis and M. J. Chappell, *Corros. Sci.*, 19 (1979) 73.
14. P. Hayfield in 'Advances in Corrosion Science and Technology', Vol. 2, Eds. M. G. Fontana and R.W. Staehle, 1972, p. 79.
15. F. C. Ho and J. L. Ord, *J. Electrochem. Soc.*, 119 (1972) 139.
16. J. O'M. Bockris, M. A. Genshaw, V. Brusic and H. Worblowa, *Electrochem. Acta*, 16 (1971) 1859.
17. A. B. Winterbottom, *J. Iron Steel Inst.* 165 (1950) 9.
18. C. E. Lederknight and B. Lustman, *J. Opt. Soc. Am.*, 29 (1939) 59.
19. D. D. MacDonald and B. Roberts, *Electrochim. Acta*, 23 (1978) 781.
20. R. S. Schrebler Guzman, J. R. Vilche and A. J. Arvia, *Electrochem. Acta*, 24 (1980) 395.